

Provided for non-commercial research and education use.
Not for reproduction, distribution or commercial use.



This article appeared in a journal published by Elsevier. The attached copy is furnished to the author for internal non-commercial research and education use, including for instruction at the authors institution and sharing with colleagues.

Other uses, including reproduction and distribution, or selling or licensing copies, or posting to personal, institutional or third party websites are prohibited.

In most cases authors are permitted to post their version of the article (e.g. in Word or Tex form) to their personal website or institutional repository. Authors requiring further information regarding Elsevier's archiving and manuscript policies are encouraged to visit:

<http://www.elsevier.com/copyright>



Combined Aharonov–Bohm and Zeeman spin-polarization effects in a double quantum dot ring

Eric R. Hedin, Abigail C. Perkins, Yong S. Joe*

Center for Computational Nanoscience, Department of Physics and Astronomy, Ball State University, Muncie, IN 47306-0505, USA

ARTICLE INFO

Article history:

Received 23 September 2010
Received in revised form 1 November 2010
Accepted 11 November 2010
Available online 13 November 2010
Communicated by R. Wu

Keywords:

Aharonov–Bohm ring
Quantum dots
Zeeman splitting
Spin-polarization

ABSTRACT

A mesoscale Aharonov–Bohm (AB) ring with a quantum dot (QD) embedded in each arm is computationally modeled for unique transmission properties arising from a combination of AB effects and Zeeman splitting of the QD energy levels. A tight-binding Hamiltonian is solved, providing analytical expressions for the transmission as a function of system parameters. Transmission resonances with spin-polarized output are presented for cases involving either a perpendicular field, or a parallel field, or both. The combination of the AB-effect with Zeeman splitting allows sensitive control of the output resonances of the device, manifesting in spin-polarized states which separate and cross as a function of applied field. In the case with perpendicular flux, the AB-oscillations exhibit atypical non-periodicity, and Fano-type resonances appear as a function of magnetic flux due to the flux-dependent shift in the QD energy levels via the Zeeman effect.

© 2010 Elsevier B.V. All rights reserved.

1. Introduction

Classical electronics exploits the electron charge to designate binary information, whereas spintronics is an emerging field in which the *spin* of the electron is used for switching purposes and to communicate information [1]. Spin-dependent effects arise from interactions of the electron with an external magnetic field or with magnetic properties of the conduction material. An important feature of an AB interferometer with a quantum dot (QD) embedded in one or both arms is the ability to probe the total spin of the electronic state of the QD. The investigation of electron-spin transport in semiconductor nanostructures and nanoscale electronic devices has attracted recent attention [2–4]. Quantum dots offer unique possibilities for manipulating and utilizing the spin of electrons in individual quantum states. The main topics of research have focused on studying the fundamental aspects of the spin-dependent transport (e.g. spin coherence times, many-body effects such as the Kondo effect or spin–charge separation [5,6], and spin-dependent tunneling [7]) and to developing and optimizing semiconductor spintronics device applications, such as spin transistors and spin qubits [2].

Experimental work [8] has shown interesting flux-dependence of the total wave function, including the spin and orbital electron configuration of the two coupled QDs. Experiments have also shown the possibility of the existence of long-lived spin states in quantum dots [2]. The spin relaxation rate in quantum dots is ex-

pected to be very low because of forbidden transitions. By this we mean that the spin of the electron can only couple to the environment indirectly through the spin–orbit coupling, which renders the spin fairly stable against random charge fluctuations [9]. The electron spin is assumed to be conserved as it tunnels in and out of the QD. Coherence, spin-decoherence, and resonant phenomena are very important for quantum computing applications. In addition, experimental demonstration of spin filtering controlled by gate voltages in a semiconductor QD has been observed [10]. Hanson et al. demonstrated clear Zeeman splitting of the two-electron triplet states of GaAs QDs by applying a large magnetic field ($B_{\parallel} = 12$ T) parallel to the plane of the 2DEG [11]. Spin–orbit interactions are negligible in their results, which minimizes mixing of the spin states, even with a large parallel field [12]. Elsewhere, it has been proposed that Fano resonances [13] associated with electron transmission through open QDs can give rise to spin polarization [14]. Our recently investigated results on sharpened AB oscillations for parallel double QDs in resonance [15] suggest another feasible mechanism for spin polarization or filtering of spin states with energy splitting. When the transmission resonance is a sharp function of energy or magnetic field, opposite electron spin states should be transmitted with a high degree of polarization.

In this article, an AB-ring with a QD embedded in each arm is analyzed for the scenario in which a perpendicular external magnetic field contributes not only an AB phase shift but also Zeeman splitting of the electron energy states in the two QDs. We investigate spin-quantum states by studying interference effects in the transmission resulting from the application of external magnetic fields to this device. In the current work, resonant transport through QDs embedded in the arms of an AB-ring is studied by

* Corresponding author.

E-mail address: ysjoe@bsu.edu (Y.S. Joe).

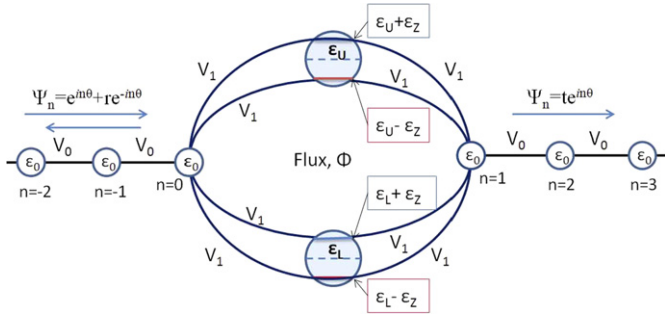


Fig. 1. (Color online.) Model of AB-ring with embedded quantum dots, showing the spin-split energy levels, $\varepsilon_U \pm \varepsilon_Z$ (upper QD) and $\varepsilon_L \pm \varepsilon_Z$ (lower QD). The spin-splitting is accomplished via the Zeeman effects by either a perpendicular flux through the entire structure, or through a parallel magnetic field.

incorporating the electron spin into the model's Hamiltonian. In these systems, the spin degeneracy of the electrons is assumed to be lifted via the Zeeman effect by the application of an external magnetic field [16]. With the spin degeneracy lifted, an energy-splitting develops between the two spin states. We demonstrate spin-polarized transmission as a result of both AB and Zeeman effects on double QDs in an AB ring. It is shown that the combination of AB and Zeeman effects produce novel transmission phenomenon such as non-periodic AB oscillations, QD-coupling-dependent dominance of either effect, and the transition from transmission resonance crossings into anti-crossings. In addition, Fano-type resonances as a function of magnetic flux appear in the transmission due to the combination of AB and Zeeman effects.

Results are presented in the form of transmission plots as a function of incident electron energy and perpendicular magnetic flux or Zeeman energy shift. We analyze both symmetric (with QD site energy values the same) and asymmetric rings. In particular, the shift of the QD energy levels due to Zeeman splitting disrupts the normal periodic modulation of the transmission seen with a pure AB-effect. In the energy spectrum of the transmission, the Zeeman effect produces spin-split transmission resonances whose separation or overlap is controlled by the applied flux. Three-dimensional contour plots of the transmission as a function of energy and flux reveal an interplay between Zeeman and AB-effects in which one or the other becomes dominant, depending on the relative magnitude of the QD-lead coupling parameter. We additionally study the transmission for an alignment of the external magnetic field parallel to the plane of the AB-ring. In this case, no AB-effect is produced, but the Zeeman splitting of the QD energy levels still produces spin-split and spin-mixed resonance states. We also show the effect of including a local perpendicular flux confined only to the center of the ring, which produces an AB-phase shift, but not any Zeeman splitting. This field can convert a crossing of the spin resonances into an anti-crossing.

2. Theoretical model and calculations

A schematic of the model used in this work is shown in Fig. 1, which illustrates the spin-split QDs in each arm of an AB-ring. The ring is coupled to semi-infinite leads which are assumed to be coupled to charge reservoirs. It is further assumed that the Zeeman splitting in the leads is negligible compared to in the QDs [11, 17,18], although our initial investigations including spin-split leads demonstrate that the main results of this work still apply. The incident and reflected electron wave functions are shown on the left and the transmitted wave function is shown on the right of the ring. The solution of the Schrödinger equation for this model gives analytical expressions for the transmission, $T = |t(E, \Phi)|^2$, and the corresponding conductance $G = \frac{2e^2}{h} T$.

The Hamiltonian for the system composed of an AB-ring with embedded QDs, coupled to one-dimensional semi-infinite leads is given in the set of equations below.

$$H_{Total} = H_{QD} + H_{QD-Leads} + H_{Leads},$$

$$H_{QD} = (\varepsilon_U + \varepsilon_Z) d_{U\downarrow}^\dagger d_{U\downarrow} + (\varepsilon_U - \varepsilon_Z) d_{U\uparrow}^\dagger d_{U\uparrow} \\ + (\varepsilon_L + \varepsilon_Z) d_{L\downarrow}^\dagger d_{L\downarrow} + (\varepsilon_L - \varepsilon_Z) d_{L\uparrow}^\dagger d_{L\uparrow},$$

$$H_{QD-Leads} = e^{i\varphi} V_1 (l_0^\dagger d_{U\uparrow} + l_0^\dagger d_{U\downarrow} + l_1^\dagger d_{L\uparrow} + l_1^\dagger d_{L\downarrow}) \\ + e^{-i\varphi} V_1 (l_1^\dagger d_{U\uparrow} + l_1^\dagger d_{U\downarrow} + l_0^\dagger d_{L\uparrow} + l_0^\dagger d_{L\downarrow}) + \text{h.c.},$$

$$H_{Leads} = \varepsilon_0 \sum_i l_i^\dagger l_i - V_0 \sum_i (l_i^\dagger l_{i+1} + \text{h.c.}), \quad (1)$$

where $d_{i\uparrow,\downarrow}^\dagger$ ($d_{i\uparrow,\downarrow}$) is the creation (annihilation) operator at upper ($i = U$) or lower ($i = L$) QDs for spin-up or spin-down electron states, ε_U and ε_L are the onsite QD energy values (without spin splitting) of the upper and lower QDs, respectively, and V_1 is the hopping probability between the QDs and the leads (assumed to be symmetric for upper and lower QDs and for left and right leads). The external magnetic field enters the Hamiltonian through the energy-shift due to Zeeman spin splitting, $\varepsilon_Z = \frac{1}{2} g \mu_B B$ and through the AB-effect. The AB phase factors, $e^{\pm i\varphi}$, introduce a phase shift to the electron wave function as a function of perpendicular magnetic flux, $\varphi = \frac{\pi\Phi}{2\Phi_0}$, where $\Phi_0 = h/e$ is the flux quantum. $l_{i\uparrow,\downarrow}^\dagger$ ($l_{i\uparrow,\downarrow}$) is the creation (annihilation) operator of each site in the leads, V_0 is the hopping probability between the sites in the leads, and ε_0 is the onsite energy of the sites in the leads. Assuming periodic wave functions in the leads allows the solution to the Hamiltonian equation to be reduced to a finite set of linear equations along with the dispersion relation, $E = -2V_0 \cos(\theta) + \varepsilon_0$, where $\theta = ka$, and a is the site spacing in the leads, and k is the wavenumber of the incident electrons.

Possible orientations of the external magnetic field with respect to the plane of the ring include a perpendicular field, \mathbf{B}_\perp , or a parallel field, \mathbf{B}_\parallel . The perpendicular field passes through the ring and the QDs and produces both the AB-effect and the Zeeman effect. The parallel field, on the other hand, will not produce any AB-effect, but will still produce Zeeman splitting of the QD energy levels.

The Zeeman effect splits the QD energy levels as $E = \varepsilon_{QD} \pm \varepsilon_Z$, where ε_{QD} is the spin-degenerate QD energy level, ε_U or ε_L . For a perpendicular field, the energy-level shift is $\varepsilon_Z = \pm \frac{1}{2} g \mu_B B_\perp$, where the value of the Bohr magneton is $\mu_B = 58 \mu\text{eV}/\text{T}$. In order to define the Zeeman energy scales which are used to calculate the transmission plots, we assume that the QDs in our system are made with bulk GaAs, which have a measured negative gyromagnetic ratio, $g = -0.44$ [19]. This value has been shown to be constant for all field directions, except for a slight variation in g for QD sizes less than about 15 nm [20]. The perpendicular magnetic field which produces the Zeeman energy splitting, ε_Z , is related in magnitude to the normalized flux $\frac{\Phi}{\Phi_0}$ as $\varepsilon_Z = 12.7 \left(\frac{\mu\text{eV}}{R}\right) \mathbf{B}_\perp = (52.7/A) (\text{meV nm}^2) \frac{\Phi}{\Phi_0}$, where A is the area of the ring in nm^2 . The magnitude of the Zeeman energy-level splitting is proportional to the external magnetic field. The value of the flux, however, (which determines the AB phase shift) depends upon the product of the field and the area of the AB ring. In the results presented below, we have assumed an AB ring radius of 200 nm, although the generality of our conclusions do not depend upon this specific value of radius. For a parallel magnetic field, we also have $\varepsilon_Z = \pm 12.7 (\mu\text{eV}/\text{T}) \mathbf{B}_\parallel$. A typical, single-level QD energy equals approximately 110 μeV [8]. The energy window for the transmission calculated with our model, as set by the dis-

persion relation with $\varepsilon_0 = 0$, is scaled according to the value of V_0 in the interval $-2.0V_0 < E < 2.0V_0$. Correspondingly, the energy scale on the transmission plots is determined by V_0 , which we set as $V_0 = 1.0$.

In order to obtain good spin-polarization in experimental devices, it is also necessary for the Zeeman energy to be larger than the thermal energy ($g\mu_B \mathbf{B}_{\parallel} \gg kT$), which is typically accomplished by performing the measurements in a dilution refrigerator at a low base temperature of 20–70 mK [10,11]. In our work, cotunneling effects are negligible due to operation in the Coulomb blockade region, which is accessed by low QD–lead coupling.

3. Results and discussion

We first consider the characteristics of the transmission in a symmetric AB ring with QDs in the presence of a perpendicular magnetic field, \mathbf{B}_{\perp} , as shown in Fig. 2. Transmission plots are shown in Fig. 3 for this case with symmetric QD energy levels set as, $\varepsilon_U = 0.5$ and $\varepsilon_L = 0.5$. The QD–lead coupling is set to $V_1 = 0.2$, except where specified otherwise. In Fig. 3a, the dashed curve shows a single transmission resonance peak at $E \approx 0.5$ due to the identical QD energy levels. At $\Phi/\Phi_0 = 0.24$, the AB phase shift and resulting interference in the output transmission produces three

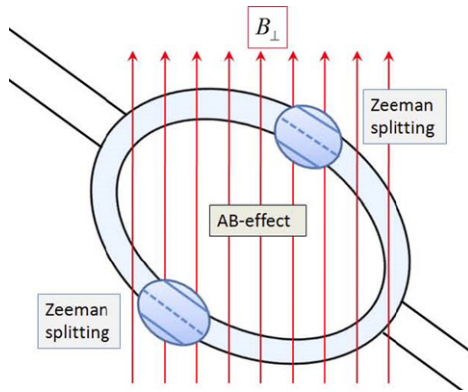


Fig. 2. (Color online.) Schematic of the AB-ring with embedded QDs, showing a perpendicular external field, \mathbf{B}_{\perp} , which causes both Zeeman splitting of the QD energy levels and an AB-effect.

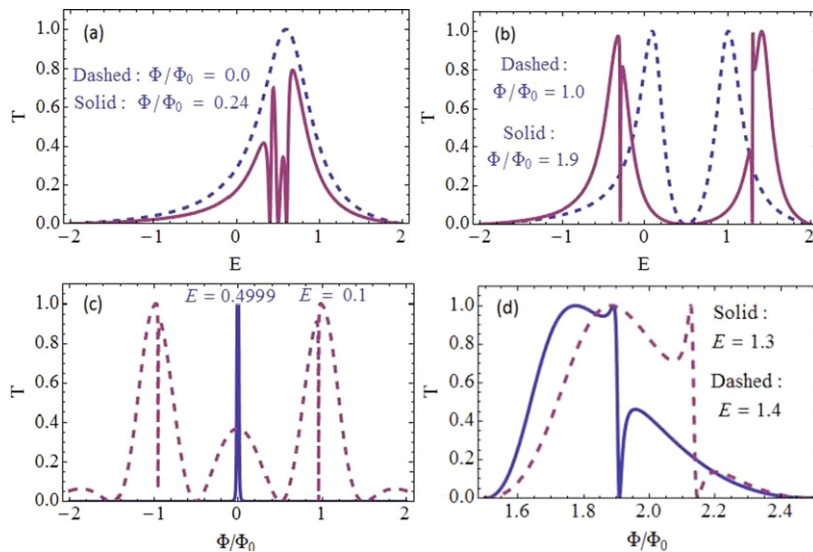


Fig. 3. (Color online.) Transmission as a function of energy for fixed flux ((a) and (b)) and as a function of flux for fixed energy ((c) and (d)). (a) Dashed curve, $\Phi/\Phi_0 = 0.0$; solid curve, $\Phi/\Phi_0 = 0.24$, (b) Dashed curve, $\Phi/\Phi_0 = 1.0$; solid curve, $\Phi/\Phi_0 = 1.9$, (c) Dashed curve, $E = 0.1$; solid curve, $E = 0.4999$, (d) Dashed curve, $E = 1.4$; solid curve, $E = 1.3$.

transmission zeros at $E = \varepsilon_U = 0.5$ and $E = \varepsilon_U \pm \varepsilon_Z$, with $\varepsilon_Z = 0.1$ for the value of applied flux.

For a symmetric double QD ring, with only one energy value, ε_U , the transmission amplitude reduces to

$$t = \{-4ie^{2i(\theta+\varphi)}V_0V_1^2\sin(\theta)(1+e^{4i\varphi}) \times [(E-\varepsilon_Z-\varepsilon_U)(E+\varepsilon_Z-\varepsilon_U)(E-\varepsilon_U)]\} \times \{4ie^{2i\theta}V_1^4(-1+e^{4i\varphi})^2(E-\varepsilon_U)^2 - 8e^{i(\theta+4\varphi)}V_0V_1^2Q(E)-e^{i4\varphi}V_0^2R(E)\}^{-1}, \quad (2)$$

where

$$Q(E) = (E-\varepsilon_Z-\varepsilon_U)(E+\varepsilon_Z-\varepsilon_U)(E-\varepsilon_U), \quad (3)$$

$$R(E) = (E+\varepsilon_Z-\varepsilon_U)^2(-E+\varepsilon_Z+\varepsilon_U)^2.$$

As is easily seen from Eq. (2), there are three transmission zeros, at $E = \varepsilon_U$ and $E = \varepsilon_U \pm \varepsilon_Z$, which appear at these energy values in the solid curve of Fig. 3a.

If $\varepsilon_Z = 0$ and $E = \varepsilon_U$, both the numerator and the denominator of the transmission amplitude go to zero, as can be seen from Eqs. (2) and (3), causing both zeros and poles in the transmission, which cancel out, leaving the single transmission resonance peak shown in the dashed curve of Fig. 3a. Fig. 3b shows two additional curves with higher values of flux, producing greater Zeeman splitting of the resonance peaks. The dashed curve is for $\Phi/\Phi_0 = 1.0$, which at this integer multiple of the flux quantum, produces only two Zeeman-split peaks without additional AB-interference resonances. The solid curve is for $\Phi/\Phi_0 = 1.9$, which shows that the AB interference effect introduces additional Fano resonances in each peak. In Fig. 3c, the combined AB and Zeeman effects produce unique transmission vs. flux curves, demonstrating a variety of non-periodic output, depending upon the value of the electron energy, E [12]. The dashed curve with $E = 0.1$ has sharp transmission zeroes at the flux values which produce a Zeeman shift of the QD energy levels to match that of the incident electron energy value. When $E = \varepsilon_U \pm \varepsilon_Z$, inspection of the transmission amplitude in Eq. (2) confirms a transmission zero. For the case with incident electron energy nearly equal to the QD site energy (shown in Fig. 3c as the solid curve labeled $E = 0.4999$), the sharp transmission spike in the solid curve at $\Phi/\Phi_0 = 0.0$ is a manifestation of AB resonance sharpening due to interference between

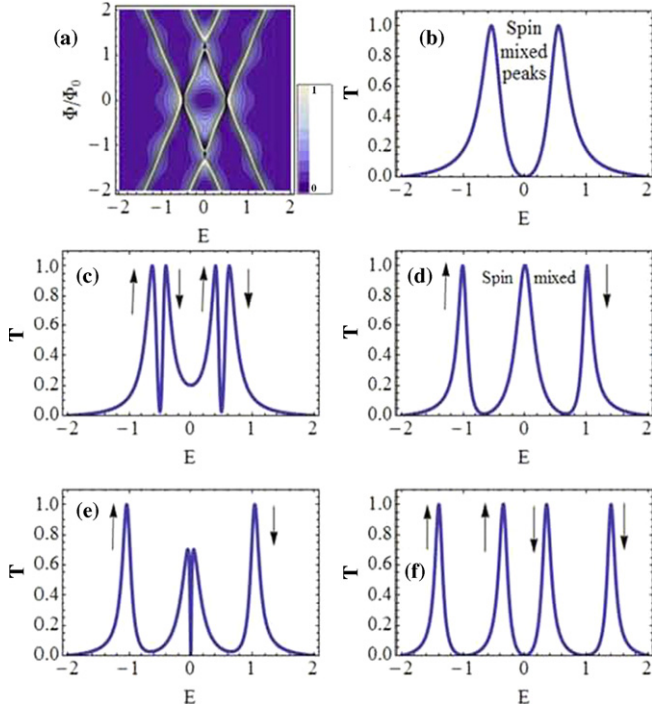


Fig. 4. (Color online.) Transmission plots for the case with $\varepsilon_U = 0.5$ and $\varepsilon_L = -0.5$, and $V_1 = 0.2$. (a) Contour plot of the transmission as a function of energy and flux. (b)–(f) Line plots of the transmission as a function of energy for increasing values of magnetic flux: (b) $\Phi/\Phi_0 = 0.0$, (c) $\Phi/\Phi_0 = 0.25$, (d) $\Phi/\Phi_0 = 1.12$, (e) $\Phi/\Phi_0 = 1.19$, (f) $\Phi/\Phi_0 = 2.0$. Arrows denote the dominant spin state of the transmission resonance.

the symmetric QD resonance levels [15]. The influence of the Zeeman effect spoils the AB resonances at all non-zero integer flux values (where they would also appear as sharp spikes without the Zeeman effect). Fig. 3d illustrates unique Fano transmission resonances as a function of magnetic flux, which arise due to the coupling between magnetic flux and QD-energy levels as a consequence of the Zeeman effect. The energy values chosen for Fig. 3d correspond approximately to the energy of the Fano resonance shown by the solid curve in Fig. 3b for $\Phi/\Phi_0 = 1.9$.

Next, we examine the coupled AB and Zeeman effects via an externally applied perpendicular magnetic field, \mathbf{B}_\perp , without any \mathbf{B}_\parallel in the AB ring with asymmetric QD energy levels. The Zeeman splitting of the QD energy states is given by $\varepsilon_Z = \pm \frac{1}{2}g\mu_B \mathbf{B}_\perp$. The perpendicular field also causes AB oscillations in the transmission which, with the added Zeeman effect, become non-periodic. The QD energy values are now anti-symmetric and set to $\varepsilon_U = 0.5$ and $\varepsilon_L = -0.5$. For QD-lead coupling of $V_1 = 0.2$, Fig. 4 shows a series of transmission plots. A contour plot of the transmission as a function of electron energy and perpendicular flux (normalized to the flux quantum, Φ_0) is shown in Fig. 4a. An increasing flux magnitude splits the QD energy levels into spin-up (lower energy) and spin-down (higher energy) resonance peaks. The spin-down state goes to higher energy due to the negative gyromagnetic ratio, $g = -0.44$, for GaAs. In Figs. 4b–f, the transmission as a function of energy is presented for progressively increasing flux values. The electron spin orientation (with respect to the external field) is indicated by the up or down arrows on the graphs. For $\Phi/\Phi_0 = 0$ (Fig. 4b), no Zeeman splitting occurs, and only two resonance peaks appear, one for each QD energy value. As the magnetic flux increases, these two peaks separate into four spin-split resonance peaks. A finite flux of $\Phi/\Phi_0 = 0.25$ produces a Zeeman splitting of the QD energy states of $\varepsilon_Z = 0.1$, which in turn produces the splitting of the resonance peaks shown in Fig. 4c. The central transmission minimum does not reach zero due to AB in-

terference effects. In Fig. 4d, at $\Phi/\Phi_0 = 1.12$, the two inner peaks have nearly overlapped, producing a spin-mixed state. In Fig. 4e, the flux value is set at $\Phi/\Phi_0 = 1.19$ which makes the Zeeman energy exactly equal to one-half the difference of the QD energy levels. This unique value produces the sharp resonance zero shown at $E = 0$ in Fig. 4e. Examination of the transmission amplitude formula for this system shows that such behavior is to be expected under these resonance conditions. At a slightly greater flux value, $\Phi/\Phi_0 = 1.30$ (not shown), the transmission again climbs to another local maximum at $E = 0$, resembling the transmission curve shown in Fig. 4d. In Fig. 4f, an even higher flux value produces larger Zeeman splitting of the resonance peaks. Now the two inner peaks have crossed over each other, reversing the order of the polarization sequence of the inner resonance peaks (compare Fig. 4c to Fig. 4f). Since the Zeeman-split QD energy states are occupied by electrons of opposite spins, the distinct transmission peaks in Fig. 4 are effectively spin-polarized. For smaller QD-lead coupling, V_1 , the transmission resonance peaks will be narrower, corresponding to increased QD confinement time as a result of the lower QD-lead coupling.

A sequence of three-dimensional plots of the transmission, with varying QD-lead coupling, as a function of E and external perpendicular flux are shown in Fig. 5. At larger QD-lead coupling, V_1 , the transmission is dominated by AB oscillations as a function of flux (Fig. 5a, with $V_1 = 0.7$), whereas for smaller V_1 , the AB oscillations weaken and the Zeeman splitting as a function of magnetic flux becomes prominent (Fig. 5d, with $V_1 = 0.2$). The transition from AB-dominated to Zeeman-dominated transmission is further seen at $V_1 = 0.5$ (Fig. 5b) and $V_1 = 0.35$ (Fig. 5c). The effect of V_1 on the dominance of the AB effect (for large V_1) or the Zeeman effect (for small V_1) can be seen in the mathematical form of the general transmission amplitude for non-identical QD energy values:

$$t = \{P(\theta, \varphi)[(E - \varepsilon_Z - \varepsilon_U)(E + \varepsilon_Z - \varepsilon_U)(E - \varepsilon_L) + e^{4i\varphi}(E - \varepsilon_U)(E - \varepsilon_Z - \varepsilon_L)(E + \varepsilon_Z - \varepsilon_L)]\} \times \{-e^{4i\varphi}V_0^2(E - \varepsilon_Z - \varepsilon_U)(E + \varepsilon_Z - \varepsilon_U)(E - \varepsilon_Z - \varepsilon_L) \times (E + \varepsilon_Z - \varepsilon_L) + O(V_1^2)e^{2i\varphi} + O(V_1^4)\}^{-1}, \quad (4)$$

where

$$P(\theta, \varphi) = -4ie^{2i(\theta+\varphi)}V_0V_1^2\sin(\theta).$$

Eq. (4) shows that for $V_1 \ll 1$, the transmission is suppressed by a factor of V_1^2 in the numerator, which leads to minimal transmission, except where $E = \varepsilon_U \pm \varepsilon_Z$ and $E = \varepsilon_L \pm \varepsilon_Z$ which maximizes the denominator and produces the narrow transmission maxima seen in Fig. 5d. The AB-oscillations are suppressed at the E -values specified above for $V_1 \ll 1$, and the Zeeman splitting behavior dominates. For example, if $E = \varepsilon_U + \varepsilon_Z$, only the second term in the numerator survives, and the main term in the denominator vanishes, leaving only a small value of the denominator, producing a transmission pole. The flux-dependent phase factor, $e^{4i\varphi}$, in the $O(V_1^2)$ term in the denominator cancels the $e^{4i\varphi}$ factor in the surviving term in the numerator. The exponential pre-factor in the numerator, given in $P(\theta, \varphi)$, always vanishes when the transmission is formed by taking the complex conjugate squared of the transmission amplitude. At E -values different from those specified above, the AB-oscillatory behavior increases. Or, if V_1 is not small compared to one, the AB-behavior then dominates over the Zeeman splitting of the QD energy values. These effects are explicitly demonstrated in the sequence of plots in Fig. 5a–d.

We next consider characteristics of the transmission in an anti-symmetric AB ring with-QDs in the presence of a magnetic field parallel to the plane of the AB ring, as shown in Fig. 6. In this

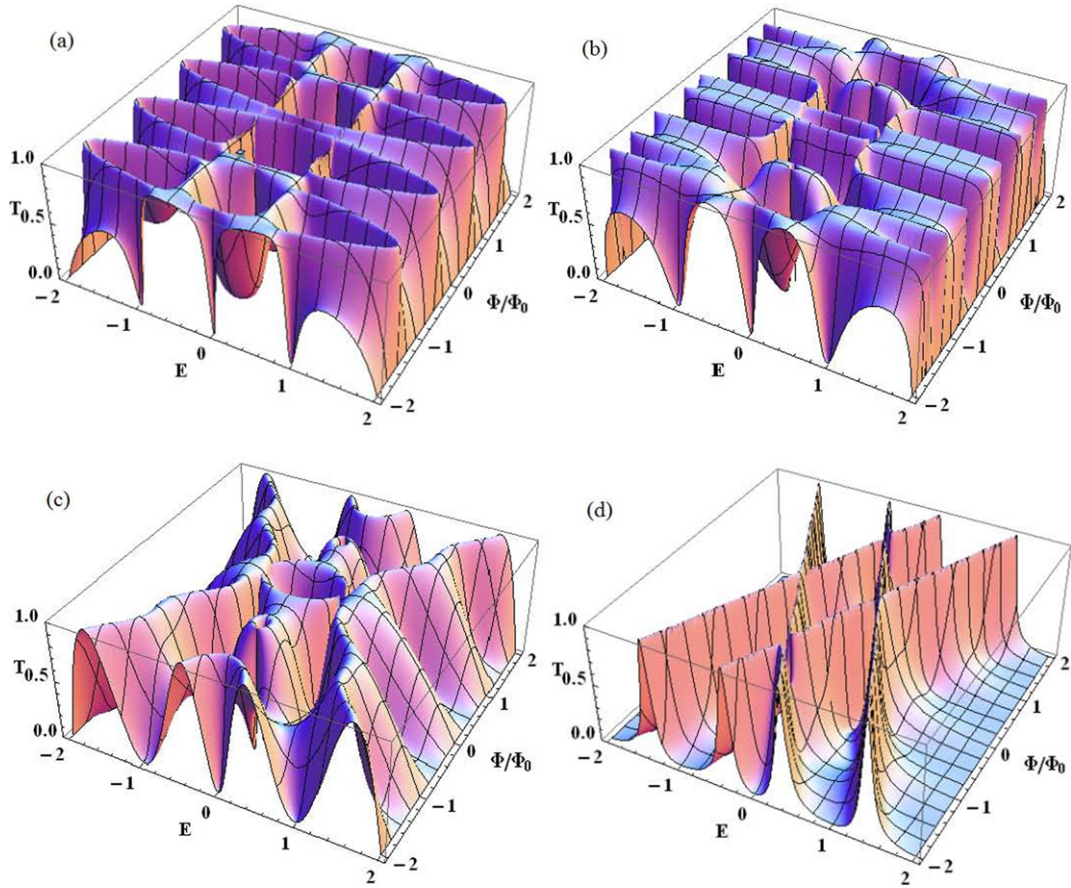


Fig. 5. (Color online.) 3D plots of transmission with decreasing ring coupling parameters V_1 [(a) $V_1 = 0.7$; (b) $V_1 = 0.5$; (c) $V_1 = 0.35$; (d) $V_1 = 0.2$] in the coupled anti-symmetric AB-ring configurations. Split QD energy levels are $\varepsilon_U = 0.5$ and $\varepsilon_L = -0.5$. The Zeeman energy $\Delta\varepsilon = 0.42\Phi/\Phi_0$.

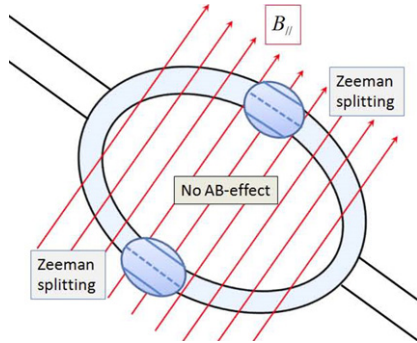


Fig. 6. (Color online.) Schematic of the AB-ring with embedded QDs, showing a parallel external magnetic field, $\mathbf{B}_{||}$, which only causes Zeeman splitting, without any AB-effect.

alternative alignment, $\mathbf{B}_{||}$ produces Zeeman splitting according to $\varepsilon_Z = \frac{1}{2}g\mu_B\mathbf{B}_{||}$, but $\mathbf{B}_{||}$ will not cause any AB effect. Fig. 7a gives a contour plot of the transmission, as a function of electron energy, E , and Zeeman splitting energy, ε_Z , due to $\mathbf{B}_{||}$. As ε_Z increases from zero, the transmission resonant peaks diverge into spin-split resonances from their initial spin-mixed states at $\varepsilon_Z = 0$ and QD energy values of $\varepsilon_U = 0.5$ and $\varepsilon_L = -0.5$. For $\varepsilon_Z = \pm 0.5$, the spin states again become mixed as the resonant peaks cross at $E = 0$. In Fig. 7b, the effect of an additional external perpendicular flux confined solely to the interior of the AB-ring is shown. Such a field only contributes an AB phase shift without causing any additional Zeeman splitting. With this flux, the transmission peak crossings seen in Fig. 7a transform into anti-crossings. Fig. 7c and

Fig. 7d show line plots corresponding to the horizontal cuts on the two contour plots, giving the conductance ($G = \frac{2e^2}{h}T$) as a function of E for values of ε_Z near the crossings and anti-crossings. The anti-crossing, due to the additional perpendicular flux, effectively creates two spin mixed states (at approximately $\varepsilon_Z = 0.42$ and $\varepsilon_Z = 0.57$) where there was only one before. The original spin-mixed state transforms into a region of suppressed conductance, as seen in the solid curve of Fig. 7d around $E = 0$.

Finally, we study the tunneling current of the system by evaluating the current-voltage (I - V) characteristics with the transmission function $T(E)$, using the standard formalism based on the scattering theory of transport [21],

$$I = \frac{2e}{h} \int dE T(E) [f_L(E) - f_R(E)]. \quad (5)$$

Here, $f(E)$ is the Fermi function given by $f_{L/R}(E) = \frac{1}{e^{\beta(E - \mu_{L/R})} + 1}$, where $\beta = 1/k_B T$ and $\mu_{L/R}$ is the electrochemical potential of the left (right) semi-infinite leads, whose values depend on the applied source-drain bias voltage V_{sd} . We assume symmetric leads and set $\mu_L = eV_{sd}/2$ and $\mu_R = -eV_{sd}/2$. In Fig. 8, we show the I - V characteristics, calculated at $T = 4$ K for the transmission (or conductance in units of $2e^2/h$) shown as solid curves in Fig. 7c and Fig. 7d. The dash-dotted I - V curve (corresponding to the case with $\Phi/\Phi_0 = 0.3$) shows smaller current for a given voltage since the additional flux suppresses the transmission near $E = 0$, as seen in Fig. 7d. Both I - V curves in Fig. 8 show current steps corresponding to the transmission resonance peaks.

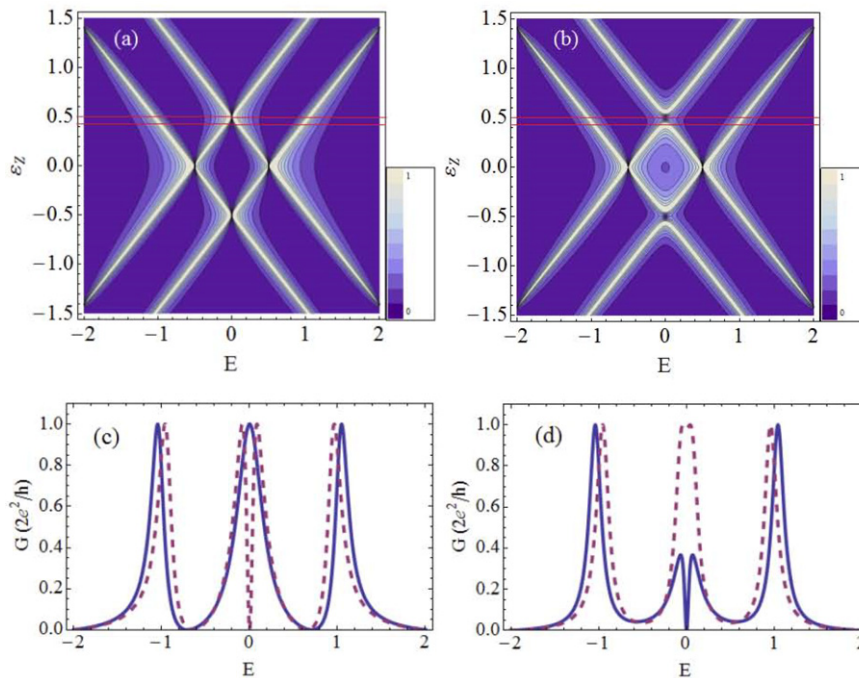


Fig. 7. Contour plots of the transmission (or conductance, in units of $2e^2/h$) with (a) $\Phi/\Phi_0 = 0.0$ and (b) $\Phi/\Phi_0 = 0.3$. (c) Line plots of the conductance with $\Phi/\Phi_0 = 0.0$ and $\varepsilon_Z = 0.5$ (solid blue), and $\varepsilon_Z = 0.42$ (dashed violet). (d) Line plots of the conductance with finite flux, $\Phi/\Phi_0 = 0.3$, confined to the interior of the AB-ring for $\varepsilon_Z = 0.50$ (solid blue) and $\varepsilon_Z = 0.42$ (dashed violet). (For interpretation of the references to color in this figure legend, the reader is referred to the web version of this Letter.)

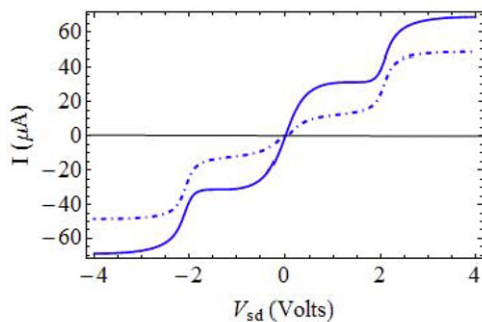


Fig. 8. (Color online.) Current vs. voltage, calculated at $T = 4$ K for the transmission (or conductance in units of $2e^2/h$) shown as solid curves in Fig. 7c and Fig. 7d. Solid I - V curve: $\Phi/\Phi_0 = 0.0$ and $\varepsilon_Z = 0.5$; dashed I - V curve: $\Phi/\Phi_0 = 0.3$ and $\varepsilon_Z = 0.5$.

4. Conclusion

We have shown the unique interplay between Aharonov–Bohm effects and Zeeman spin splitting on the transmission through an AB-ring with embedded QDs. Via the Zeeman effect, the QD energy levels are coupled to the external magnetic field, giving rise to Fano-type resonances as a function of magnetic flux. Additionally, the shift of the QD energy levels due to Zeeman splitting disrupts the normal periodic modulation of the transmission seen with a pure AB-effect. Either the AB-effect or the Zeeman spin-splitting effect can be made dominant in the transmission output, depending on the relative magnitude of the QD–lead coupling parameter. Analysis of the transmission amplitude shows explicitly the interplay between these two effects. With the inclusion of both a parallel field and a perpendicular field which is confined to the interior of the AB-ring, an anti-crossing of the spin-polarized states develops which leads to two diverging spin-mixed resonance states, separated by a region of suppressed transmission which re-

duces the current flow through the device at a given source-drain voltage. Overall, these studies have illustrated the effects of the combination AB effects and Zeeman spin-splitting in a double QD AB ring. Possible applications for spintronics include spin-polarized transmission and unique magnetic field-dependent control over spin-resonance states.

References

- [1] S.A. Wolf, D.D. Awschalom, R.A. Buhrman, J.M. Daughton, S. von Molnár, M.L. Roukes, A.Y. Chtchelkanova, D.M. Treger, *Science* 294 (2001) 1488.
- [2] I. Zutic, J. Fabian, S. Das Sarma, *Rev. Mod. Phys.* 76 (2004) 323.
- [3] J.C. Chen, A.M. Chang, M.R. Melloch, *Phys. Rev. Lett.* 92 (2004) 176801.
- [4] J. Zhou, M.W. Wu, M.Q. Weng, *Phys. Lett. A* 349 (2006) 393.
- [5] A.G. Aronov, G.E. Picus, *Sov. Phys. Semicond.* 10 (1976) 698.
- [6] U.F. Keyser, C. Fuhner, S. Borck, R.J. Haug, M. Bichler, G. Abstreiter, W. Wegscheider, *Phys. Rev. Lett.* 90 (2003) 196601.
- [7] A.M. Satanin, *Sov. Phys. Solid State* 31 (1989) 1497.
- [8] A.W. Holleitner, C.R. Decker, H. Qin, K. Eberl, R.H. Blick, *Phys. Rev. Lett.* 87 (2001) 256802.
- [9] W.A. Coish, D. Loss, *Phys. Rev. B* 75 (2007) 161302(R).
- [10] J.A. Folk, R.M. Potok, C.M. Marcus, V. Umansky, *Science* 299 (2003) 679.
- [11] R. Hanson, L.M.K. Vandersypen, L.H. Willems van Beveren, J.M. Elzerman, I.T. Vink, L.P. Kouwenhoven, *Phys. Rev. B* 70 (2004) 241304(R).
- [12] M. Hentschel, H. Schomerus, D. Frustaglia, K. Richter, *Phys. Rev. B* 69 (2004) 155326.
- [13] U. Fano, *Phys. Rev.* 124 (1961) 1866.
- [14] J.F. Song, Y. Ochiai, J.P. Bird, *Appl. Phys. Lett.* 82 (2003) 4561.
- [15] E.R. Hedin, Y.S. Joe, A.M. Satanin, *J. Comput. Electron.* 7 (2008) 280.
- [16] V. Kashcheyevs, A. Schiller, A. Aharony, O. Entin-Wohlman, *Phys. Rev. B* 75 (2007) 115313.
- [17] P. Recher, E.V. Sukhorukov, D. Loss, *Phys. Rev. Lett.* 85 (2000) 1962.
- [18] P. Zhang, Q.-K. Xue, X.C. Xie, *Phys. Rev. Lett.* 91 (2003) 1966602.
- [19] R.M. Potok, J.A. Folk, C.M. Marcus, V. Umansky, M. Hanson, A.C. Gossard, *Phys. Rev. Lett.* 91 (2003) 016802.
- [20] E. Reyes-Gómez, N. Porrás-Montenegro, C.A. Perdomo-Leiva, H.S. Brandi, L.E. Oliveira, *J. Appl. Phys.* 104 (2008) 023704.
- [21] S. Datta, *Quantum Transport: Atom to Transistor*, Cambridge University Press, New York, 2005.